Exploring debris-flow history and process dynamics using an integrative approach on a dolomitic cone in western Austria

Emily Procter,[1] Markus Stoffel,[1,2]* Michelle Schneuwly-Bollschweiler[1,2] and Mathias Neumann[1,3]
[1] Laboratory of Dendrogeomorphology, Institute of Geological Sciences, University of Berne, Berne, Switzerland
[2] Climatic Change and Climate Impacts, Environmental Sciences, University of Geneva, Carouge-Geneva, Switzerland
[3] Institute of Mountain Risk Engineering, University of Natural Resources and Applied Life Sciences, Vienna, Austria

ABSTRACT: The evolution of a debris-flow cone depends on a multitude of factors in the hydrogeomorphic system. Investigations of debris-flow history and cone dynamics in highly active catchments therefore require an integrative approach with a temporal and spatial resolution appropriate for the goals of the study. We present the use of an orthophoto time series to augment standard dendrogeomorphic techniques to describe the spatio-temporal dynamics of debris flows on a highly active cone in the western Austrian Alps. Analysis of seven orthophotos since 1951 revealed a migration of active deposition areas with a resulting severe loss of forest cover (> 80%) and a mean tree loss per year of 10·4 (range 1·3–16·6 trees per year). Analysis of 193 *Pinus mugo* ssp. *uncinata* trees allowed the identification of 161 growth disturbances corresponding to 16 debris flows since 1839 and an average decadal frequency of 0·9 events. As a result of the severe loss of forest cover, we speculate that < 20% of the more recent events were actually captured in the tree-ring record, giving a decadal return interval of ~7·5 events for a period of 60 years. Based on three annual field observations, it is evident that this catchment (the *Bärenrüfe*) produces very frequent (< 1 yr), small (in the order of a few 10 to 100 m³) debris flows with minor material relocation. The specific challenges of tree-ring analysis in this tree species and in highly active environments are explicitly addressed in the discussion and underline the necessity of employing complementary methods of analysis in an integrative manner. Copyright © 2012 John Wiley & Sons, Ltd.

KEYWORDS: debris flow; dendrogeomorphology; tree rings; orthophoto; Austrian Alps

Introduction

Depositional cones are a common feature in mountainous landscapes and reflect the complex hydrogeomorphic processes occurring in their catchments (Stoffel and Wilford, 2012). A comprehensive characterization of cone morphology is important for a basic understanding of process dynamics at a site as well as for the reconstruction of mass-movement events, and has implications for natural hazard management. In the past, investigations of large- and fine-scale features on debris-flow cones have been used to differentiate process types (Volker *et al.*, 2007), define specific parameters such as surface roughness (Staley *et al.*, 2006), or analyse historical events (Blair and McPherson, 1998). Relying solely on field inspection and present-day cone morphology is insufficient to properly characterize torrent history or patterns of event frequency and an integrative approach that can provide information retrospectively on events and cone development is required. A variety of methods have been used in investigations of cone morphology and torrent history, including analysis of historical records (Marchi and Tecca, 2006; Marchi and Cavalli, 2007), integrative geomorphic

mapping (Theler *et al.*, 2010) and mapping of surface morphology using airbone LiDAR (Light Detection and Ranging; Cavalli and Marchi, 2008; Cavalli *et al.*, 2008; Scheidl *et al.*, 2008). The vegetation structure on a cone can also be used as an indicator of process history (Baroni *et al.*, 2007). Caution must be taken, however, that both the temporal and spatial resolution of the methods is appropriate for the aims of the investigation.

Dendrogeomorphology is a technique of reconstructing historical mass-movement events (e.g. debris flows) through growth disturbances contained in tree rings (Alestalo, 1971; Stoffel *et al.*, 2010). As tree-ring series provide a continuous record over the lifespan of the tree (or, collectively, over the lifespan of the sampled population), this approach offers high, i.e. monthly to annual, temporal resolution (Stoffel *et al.*, 2008b). However, as dendrogeomorphology is limited to the available tree population and as tree survival in active debris-flow areas is often low, the method has a limited spatial resolution. Aerial photographs, however, provide a much higher spatial resolution but a temporal resolution that is limited to one specific moment in the past or one period, depending on the number of available photographs.

We propose that integrating orthophoto interpretation with dendrogeomorphic techniques would provide a picture of cone morphology at a high spatial resolution and a record of past debris-flow activity at a high temporal resolution. The aim of this study is (i) to document the use of a time-series of orthophoto information to support a dendrogeomorphic analysis of debris-flow history on a highly active debris-flow cone, and (ii) to highlight the effect of severe tree loss on reconstructed tree-ring analyses.

Study site

This study investigated the Bärenrüfe torrent located in the westernmost reaches of the Northern Calcareous Alps in the province of Vorarlberg, Austria (47°5′N, 9°38′E, Figure 1). The Bärenrüfe extends from 2380 m above sea level (a.s.l.) to its confluence with the Meng River at 1190 m a.s.l. (Figure 1). The dominant geological material in the catchment is limestone or dolomite (Permian to Lower Cretaceous; Geologische Bundesanstalt, 2000). The upper catchment is composed of a network of collecting and transport channels and extends from 2380 m a.s.l. to the cone apex at 1350 m a.s.l. with a total area of 0·54 km^2 and a mean slope of 58°. The cone has an average slope of 17° and a length of 480 m. The area of the primary cone is 0·05 km^2 and the area of the secondary, older deposits is 0·15 km^2.

The vegetation in the upper catchment (1400–2000 m a.s.l.) is composed of shrubs and grasses (*Seslerio-Semperviretum* plant associations). In lower regions, *Pinus mugo* ssp. *uncinata* (PIUN) have a competitive advantage on these dry, matrix-poor debris-flow deposits (Mayer, 1974) and form almost homogeneous stands on the cone. *Picea abies* (L.) Karst. (PCAB) trees are found alongside PIUN trees towards the lateral borders of the cone and compose nearly homogeneous forests outside of active depositional areas (Figure 1).

The investigated sub-sectors on the Bärenrüfe cone are shown in Figure 2. The upper, northern sector (sector A) is composed of old deposits which have been re-vegetated with grasses. This sector is only sparsely populated with PIUN trees. The lower, northern area (sector B) is the most active sector with frequent depositional events and severe burial stress on existing trees. The forest coverage is greater than in sector A and has areas of both homogenous PIUN stands and mixed PIUN-PCAB stands. The lower, southern sector (sector C) is composed of multiple, older lobate deposits which have not been re-vegetated. Forest coverage is limited to singular or small groupings of PIUN trees here.
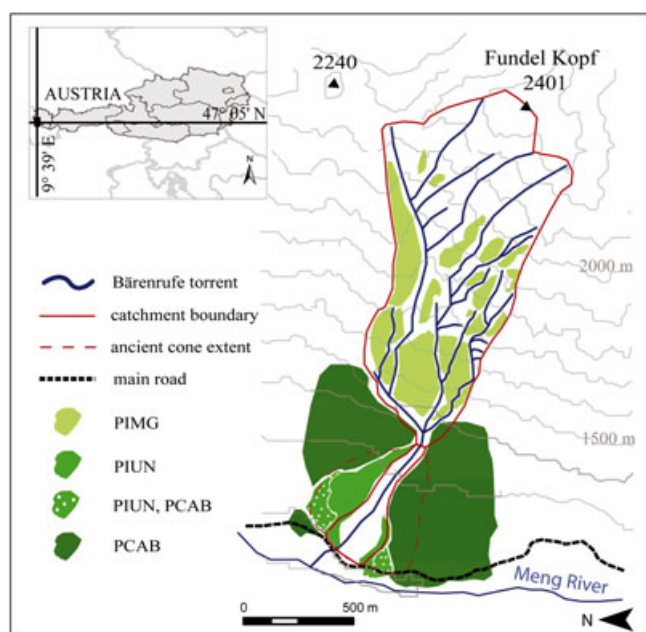
Debris flows in this catchment can be classified as granular flows with low water content and typical grain sizes between 5 and 20 cm with instances of larger material, especially near the cone apex. Archival records of the local farming association and the Austrian Federal Service for Torrent and Avalanche Control (WLV) contain descriptions of only four past debris-flow events, including 1948, 1979, 1991, and 1999. The climate in this valley is cool and humid with an average annual precipitation of 1720 mm (mean for the period 2000–2009; Hydrographischer Dienst Vorarlberg, 2010) measured at a meteorological station 2·5 km south of the Bärenrüfe torrent in Nenzinger Himmel (47°5′N, 9°38′E, 1370 m a.s.l.). Anthropogenic influence in this area is limited to occasional road maintenance and recreational hunting.

Methods

Orthophoto analysis

The official archives contained a total of seven orthophotos derived from aerial photographs that have sufficient resolution for analysis: 30 August 1951 (25 cm), 15 August 1973 (25 cm), 1 October 1987 (50 cm), 25 August 2001 (25 cm), 29 August 2005 (25 cm), 20 September 2006 (12 cm) and 26 July 2009 (12 cm) (Land Vorarlberg, 2010). Orthophotos were analysed with ArcMap 9.3 Software (ESRI, 2008) to enable accurate spatial comparison. Analysis focused on the following parameters: (i) spatial extent of active depositional areas; (ii) course and width of the main channel on the upper cone; (iii) areas of channel incision; (iv) avulsion locations; (v) spatial extent of forested and otherwise vegetated areas; and (vi) number of trees in areas of active deposition. For the spatial extent of active depositional areas, the age of deposits relative to each other was inferred from shading in the photographs, as the borders between darker (i.e. older) and lighter (i.e. younger) deposits were distinct in all cases. For the comparison of spatial extent and tree count in forested areas, the focus was limited to those areas on the primary cone which have been most influenced by debris-flow activity over the investigated time period; heavily forested areas lateral to the cone were not considered. For these comparisons, the desired areal extent was defined in ESRI ArcMap and applied to each orthophoto to ensure the exacting of locations.

Dendrogeomorphic analysis

Field investigations took place in July 2009, 2010, and 2011 to identify geomorphic processes present in different areas of the catchment, to monitor changes in superficial cone morphology within a 1-yr period and to obtain tree samples for dendrogeomorphic analysis. Trees were selected based on exposure to past debris-flow activity (for details see Stoffel and Bollschweiler 2008, 2009a, and references cited therein). A minimum of two increment cores were extracted per tree, with one in the assumed direction of past flow events and

Figure 1. Location of the investigated torrent in the western province of Austria (inset) and schematic of the Bärenrüfe catchment highlighting present forest structure (PIMG, *Pinus mugo*; PIUN, *Pinus mugo* ssp. *uncinata*; PCAB, *Picea abies*). This figure is available in colour online at wileyonlinelibrary.com/journal/espl
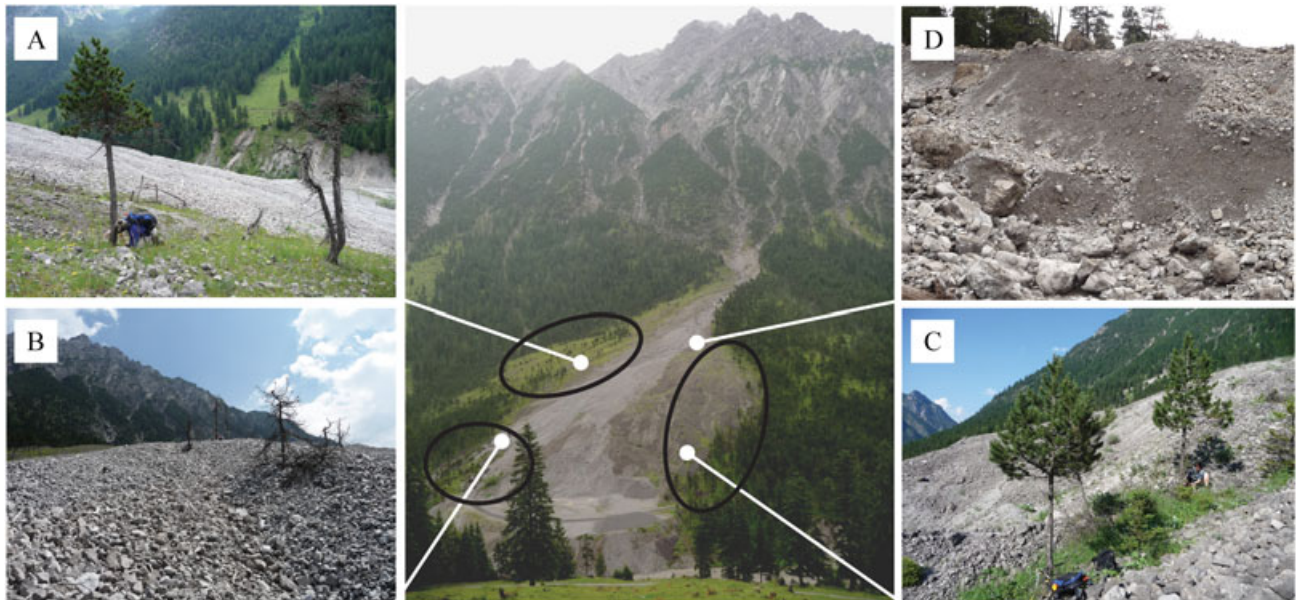
Figure 2. Characteristic sub-sectors on the debris-flow cone. Sector A is comprised of singular trees in an older, inactive deposit (A), sector B is currently the most active area where deep burial is causing rapid tree die-off (B), sector C is comprised of groupings of trees in moderately old deposits (C), and the transport channel in the upper cone area (D) shows incision depths of up to 3 m. Areas sampled for the dendrogeomorphic analysis are designated A, B, and C corresponding to these sub-sectors (circles). This figure is available in colour online at wileyonlinelibrary.com/journal/espl

one in the opposite direction. Cores were taken as low as possible for buried stems or in the area of non-vertical growth for tilted stems. For trees with visible scars, either additional cores or wedges were taken laterally to the over-walling callus tissue. Stem cross-sections were made from dead trees. In total, 193 PIUN trees were sampled from three sectors giving a total of 310 increment cores, 45 cross-sections and two wedges (Table I; data from five sampled PCAB trees were excluded from this analysis). The mean age of the samples is 144 ± 75 yr (1866) with an age range between 450 and 43 yr (1560–1967). The oldest trees are located in sector A (198 ± 65 yr), followed by sector B and C (132 ± 66 yr and 122 ± 71 yr, respectively).

The preparation and analysis of samples followed standardized dendrogeomorphic procedures as described in Stoffel and Bollschweiler (2008, 2009a). Ring-width measurements were made with a digital LINTAB positioning table with an adjoining Leica stereomicroscope and the time-series analysis software TSAP 6.43 (Time Series Analysis and Presentation;

Rinntech, 2011). Resulting measurements were graphically and statistically compared with a reference chronology, which was created using a spline function in TSAP, and missing or false rings were corrected where necessary. As PIUN trees in this region are not found outside the extent of the active cones, it was not possible to sample 'undisturbed' trees for the purpose of a reference chronology. The reference chronology was therefore produced from a sub-sample of 20 trees (40 increment cores) growing on the cone that did not exhibit highly varied growth or severe growth disturbances (GDs) in their tree-ring series. All samples were visually inspected under a stereomicroscope to identify GD associated with geomorphic disturbances, including abrupt growth suppression or release, compression wood and injuries (for details see Stoffel and Bollschweiler, 2008, 2009a).

As reactions of PIUN to debris-flow disturbances have not been documented for an equivalent site or flow process, the identification of GDs related to past debris-flow events

Table I. Description of the sample obtained for the dendrogeomorphic analysis

Sector	Trees	Samples		Sampled age	Years	Date
A	49	Cores	105	Mean	198	1812
		Cross-section	0	Standard deviation	65	—
		Wedges	0	Range (maximum/minimum)	364/70	1646/1940
		Total	105			
B	62	Cores	55	Mean	132	1878
		Cross-section	36	Standard deviation	66	—
		Wedges	1	Range (maximum/minimum)	372/47	1638/1963
		Total	92			
C	82	Cores	150	Mean	122	1888
		Cross-section	9	Standard deviation	71	—
		Wedges	1	Range (maximum/minimum)	450/43	1560/1967
		Total	160			
Total	193	Cores	310	Mean	144	1866
		Cross-section	45	Standard deviation	75	—
		Wedges	2	Range (maximum/minimum)	450/43	1560/1967
		Total	357			

Note: The location of sectors A, B and C are shown in Figure 2.

followed a three-step process. Firstly, the type and intensity of GDs were examined for years of known historical events (e.g. 1948, 1991) and all samples were compared for similar patterns of GDs. Secondly, abrupt changes in tree growth (i.e. increase or decrease relative to previous years) were only accepted as meaningful if they differed in direction and/or magnitude from the sample reference chronology. Thirdly, all GDs were then assigned to an intensity class (T_w, weak, T_m, intermediate and T_s, strong signals, and T_i, injuries) following the approach of Kogelnig-Mayer *et al.* (2011). The criteria for this classification are shown in Table II.

For the identification of events, it is essential to consider equally the spatial distribution and number of trees containing GDs in concurrent years as well as the intensity of reactions. The W_{it} index (Kogelnig-Mayer *et al.*, 2011) is an extension of the index value proposed by Shroder (1978) or Butler and Malanson (1985) which integrates the intensity in addition to the number of trees containing GDs:

$$W_{it} = \left(\left(\sum_{i=1}^{n} T_i * 7 \right) + \left(\sum_{i=1}^{n} T_s * 5 \right) + \left(\sum_{i=1}^{n} T_m * 3 \right) + \left(\sum_{i=1}^{n} T_w \right) \right) * \frac{\sum_{i=1}^{n} R_t}{\sum_{i=1}^{n} A_t}$$

where the weighting factor of seven, five, three and one are multiplied by the sum of trees containing GDs of decreasing intensity ($T_i > T_s > T_m > T_w$), respectively. This is multiplied by the ratio of number of trees containing a GD in year t (R_t) by the total number of trees alive in year t (A_t). The result is a weighted index for the given event year which can be used in combination with the spatial distribution of affected trees to identify events. A definitive index threshold does not exist, as values are highly subject to the local flow process, flow properties and tree species (Butler and Malanson, 1985; Kogelnig-Mayer *et al.*, 2011). For the purpose of this study, the threshold for an event to be accepted was set to $W_{it} \geq 0.99$ and values lower than this were excluded unless the spatial distribution of affected trees were localized and plausible. Finally, as growth suppression and release reactions can be delayed in PIUN following a disturbance, we focused on injuries or abrupt growth changes prevailing in one year, and GDs in subsequent years were considered if there was additional supporting evidence (e.g. tree location).

Results

Orthophoto interpretation of cone dynamics

The spatial extent of active areas of deposition was determined for all seven orthophotos. Between 1951 and 2009, the flow of material and overall depositional patterns could be divided into three phases (Figure 3). The first phase (Figure 3A) is visible in

the orthophotos from 1951 and 1979 – deposition of material occurred in two flow paths, which divided in the lower cone area at *c.* 1230 m a.s.l. In 1951, deposits reached well over the main road, which was itself clear of deposits, and flow paths extended into the forested areas of sector B and C. Avulsions out of the main channel at *c.* 1270 m a.s.l. also created minor flow paths into sector A. The patterns of flow were similar in 1973, but the distal extent of depositions was *c.* 100 m less than in 1951. The second phase (Figure 3B) is visible in the orthophotos from 1987 and 2001 – the flow path was directed northward, concentrating depositions in forested areas of sector B. The orthophoto from 1987 shows an avulsion location at 1270 m a.s.l., which affected trees in the central, lower area of sector A, and an avulsion at 1260 m a.s.l. created a small depositional arm in the upper section of sector C. Furthermore, an incision in the transport channel at 1240 m a.s.l. (which was also visible in 1951 and created the northern flow path at that time) continued to redirect the flow path further northward into sector B. The northern extent of active depositional areas in 2001 was *c.* 35 m further northward compared to the first phase. The third phase (Figure 3C) is visible in the orthophotos from 2005, 2006 and 2009 – avulsions between *c.* 1240–1260 m a.s.l. reactivated a south-central flow path. A large event in 2005 caused an avulsion out of the previous transport channel, bringing large depositional masses to the lower, central cone area and the road. This south-central flow path was again active in 2006 and 2009. Sector B was also affected by heavy deposits in these two years and the northern extent of deposits in 2009 were *c.* 50 m further into sector B compared to 1951 (Figure 4).

A quantitative description of active depositional areas for each available year is shown in Table III. The depositions seen in 1951 had the greatest values for areal coverage, maximum length and upper channel width. Areal coverage and maximum length of deposits show an increase between 1973 and 2009, but do not exceed the values of 1951. The transport channel in the uppermost area of the cone migrated *c.* 10–15 m southward between 1951 and 2009, eroding the southern bank and creating a current incision depth of up to 3 m. The overall width of the active channel here has decreased *c.* 25–30 m since 1951.

Forest coverage

The resolution of the orthophotos was high enough to distinguish single trees, enabling a tree count for individual years. Only the extent of the exposed cone area in the 2009 orthophoto was considered (see tree extent in Figure 4B). Overlaying this extent on previous orthophotos, a comparison of tree coverage was possible (Table IV). Tree loss ranged between 2·9% for a 4-yr period (i.e. 2001–2005) and 48·8% for a 14-yr period (i.e. 1973–1987), which corresponds to a net tree loss per year of 1·3 and 16·6 trees, respectively. Tree loss over the period 1951–2009 was over 80%, which corresponds to a net

Table II. Criteria for the classification of growth disturbance intensity as weak (T_w), moderate (T_m), strong (T_s) and injuries (T_i)

		T_w	T_m	T_s	T_i
Growth suppression and release	Change in tree-ring width (%)	< 60	≥ 60	≥ 60	
	Duration (years)	≥ 2	≥ 2 to < 5	≥ 5	
Compression wood	Cellular composition	≥ 50% of ring width consists of compression wood cells			
	Duration (years)	≥ 2	≥ 3 to < 5	≥ 5	
Injury					Presence of callus tissue or injury

Note: adapted from Kogelnig-Mayer *et al.*, 2011.
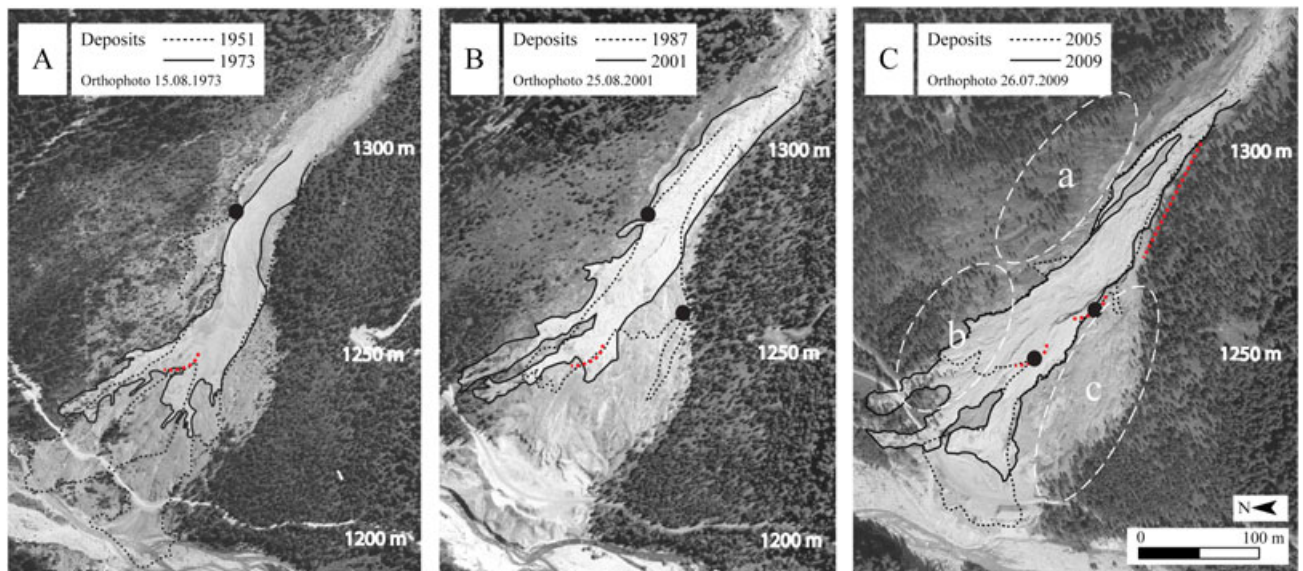
Figure 3. Evolution of active depositional areas in three phases since 1951 based on archival orthophotos. Active depositional areas included two main flow paths between the 1950s and 1970s (A). This was reduced to activity primarily in the northern path between the 1970s and 2001 (B), but avulsion out of the primary channel at *c.* 1250 m a.s.l. reactivated the south-central flow path in 2005 and both areas continue to be active (C). Avulsion locations (●), areas of channel incision (dashed line) and sampled sectors (a, b and c) are indicated (orthophotos are property of Land Vorarlberg, 2010). This figure is available in colour online at wileyonlinelibrary.com/journal/espl
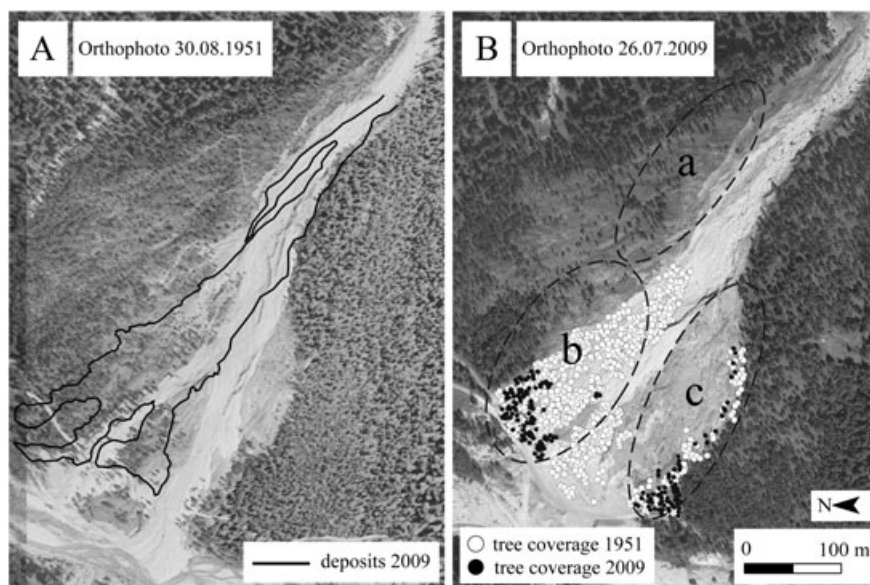
Figure 4. Comparison of active depositional areas and forest coverage between 1951 and 2009. Current depositions extend *c.* 50 m further northward into areas that were densely forested in 1951 (A), inducing an overall tree loss in the area of the 2009 deposits of *c.* 90% (B). Sampled sectors (a, b and c) are indicated (orthophotos are property of Land Vorarlberg, 2010).

loss per year of 10·4 trees. The majority of tree loss occurred in the central cone area and in sector B. Considering only the central forested area (located between depositional arms in 1951), tree loss was 100% by 2001 (tree count 1951: 140; 1973: 41; 1987: 6; 2001: 0). The migration of deposition further northward into sector B caused significant tree loss as well; when considering only the extent of the 2009 deposits (Figure 4), tree loss between 1951 and 2009 was almost 90% (1951: 538; 2009: 51). An additional area that experienced a high rate of tree loss over a short span was the lower, inner area of sector A, where an increase of activity between 1973 and 1987 caused a loss of 115 trees.

The overall forest coverage in sector A showed a constant decrease since 1951, which, given the absence of debris-flow activity in the outer extents of this area, may be attributable to poor growing conditions. Tree loss within the span of 1 yr was

noticeable in sector B. A comparison of the 2005 and 2006 orthophotos revealed a disappearance of at least 12 trees in the central area of sector B. Similarly, both a disappearance of trees and a rapid progression of needle discolouration/loss were apparent for trees in this same area between field trips in 2009, 2010, and 2011. And finally, tree coverage in sector C has not changed greatly apart from some loss on the lower, innermost area due to debris-flow activity in the first and third depositional phases.

Types of growth disturbances related to debris-flow activity

GDs in years of well-documented events were examined first. The most evident event was that of 1991, in which a total of

Copyright © 2012 John Wiley & Sons, Ltd.

Earth Surf. Process. Landforms, Vol. **37**, 913–922 (2012)

Table III. Depositional characteristics based on information in archival orthophotos

Year	Depositional area (km^2)	Maximum length of deposits from cone apex (m)	Channel width in upper cone area (m)	Avulsion locations (m a.s.l.)
1951	0·025	560	45	1240, 1270, 1280
1973	0·012	485	24	—
1987	0·013	438	24	1260, 1270
2001	0·016	487	44	—
2005	0·021	555	42	1240–1260
2006	0·020	543	42	—
2009	0·021	550	18	—

Note: The cone apex is found at 1380 m a.s.l. and the upper channel width was measured at 1300 m a.s.l.

Table IV. Degree of tree loss measured for years with orthophoto records

Year	Existing trees	Tree loss since previous measurement		
	Count	Count	Percentage	Count/year
1951	746	—	—	—
1973	475	271	36.3	12.3
1987	243	232	48.8	16.6
2001	173	70	28.8	5.0
2005	168	5	2.9	1.3
2006	156	12	7.1	12.0
2009	143	13	8.3	4.3
Since 1951	—	603	80.8	10.4

Note: The spatial extent in consideration is limited to the main cone area, as shown in Figure 4B.

16 trees contained six injuries, five abrupt growth releases, four abrupt growth suppressions and one case of compression wood.

An example of GD related to the 1991 event for two trees is shown in Figure 5A. The growth suppression seen in the tree ring is even more evident in the growth curve. The second tree shows a common pattern of growth suppression in the year following the event and the onset of compression wood and growth increase thereafter, which is also evident in the growth curve. For the GD related to the 1991 event, a delayed onset of 0 to 2 yr was seen in the case of growth suppression and 0 to 3 yr for growth release. The event of 1948 was recorded in the tree-ring series of 13 trees as 10 growth releases and three growth suppressions. A delayed onset of 0 to 1 yr was seen in the case of growth suppression and 0 to 3 yr for growth release.

All samples were then examined for similar patterns of GDs in other years. Figure 5 shows the reconstructed events of 1934 and 1851 as examples of identified GDs in other years. The event of 1934 was recorded in trees in sector C in the form of growth suppression ($n = 4$) and compression wood ($n = 1$). In both cases shown, the growth suppression is visible in both the tree rings and the growth curves. The event of 1851 was recorded in trees in sector A and C in the form of growth release ($n = 4$) and compression wood ($n = 2$). The increase in ring width in the year(s) following the event is obvious in the growth curves and contrasts the growth pattern seen in the reference curve.

In total, the analysis of the 310 samples resulted in 161 GDs related to past debris-flow activity (Table V). Abrupt growth release was the most frequently identified GD (117, 72·7%), followed by abrupt growth suppression (28, 17·4%), injuries (nine, 5·6%) and compression wood (seven, 4·3%). For each event, the predominance of one type of GD was often seen (e.g. 1839, 1922, 1981) and combinations of GD types were less frequent (e.g. 1991, 1998, 2003). The corresponding average W_{it} index was 5·3 (range 0·60–16·0; Table V), and years containing GDs that were not identified as event years had a mean W_{it} value of 0·2 (range 0·01–0·38). Two events with a $W_{it} \leq 0·99$ have been declared possible events based on an assessment of the reaction and spatial distribution of the trees.

Similar to the control events of 1991 and 1948, the onset of compression wood was either in the year of the event or in the following year, depending on the seasonal timing of the disturbance. However, the onset of growth suppression and release was often delayed, for which reason events were only identified for those cases with additional supporting evidence (see Methods section). For abrupt growth suppression, 85·7% of cases had an onset in the year of the event or in the following year, whereas 14·3% had a delayed onset of 2 to 3 yr. Similarly, the majority of cases of growth release showed an onset in the year of the event or in the following year (59·3%), but 40·7% showed a delay of 2 to 4 yr.

Event frequency

The 161 GDs allowed identification of 16 debris-flow events between 1839 and 2010 (Figure 6). Identification of GDs from the seventeenth and eighteenth centuries was possible; however, a limited sample depth during this period inhibited a reliable determination of events and these years were not reported. Considering the time period since 1839, the overall return period (i.e. the average number of years between events) is 10·7 yr and the mean decadal frequency is 0·9 events. Debris-flow frequency shows an increase since the 1960s with nine of the 16 identified events occurring within this period. The overall return interval for the past five decades is 5·5 yr, with a mean decadal frequency of 1·8 events.

Comparison of orthophoto analysis and tree-ring data

A comparison of results showed that the distribution of trees showing GDs generally corresponded to the depositional patterns seen in the most relevant orthophoto (i.e. the photo nearest to the event year). The affected trees in any event were either (i) completely contained within the distal deposits of main flow paths (e.g. events of 1961, 1968 and 2007), (ii) partially contained within the lateral aspects of distal deposits (e.g. events of 1981 and 2003) or (iii) located directly below avulsion locations (e.g. the event of 1948 in sector A and the event of 1987 in sector C). The tree-ring data offered additional information on debris-flow activity that was not obvious in the orthophotos. For example, the event of 2003 contained affected trees in sector C where new depositions were not visible in either the 2001 or 2005 orthophotos, but where small gullies were apparent in the old depositions. These gullies presumably supported water transportation and/or material relocation,
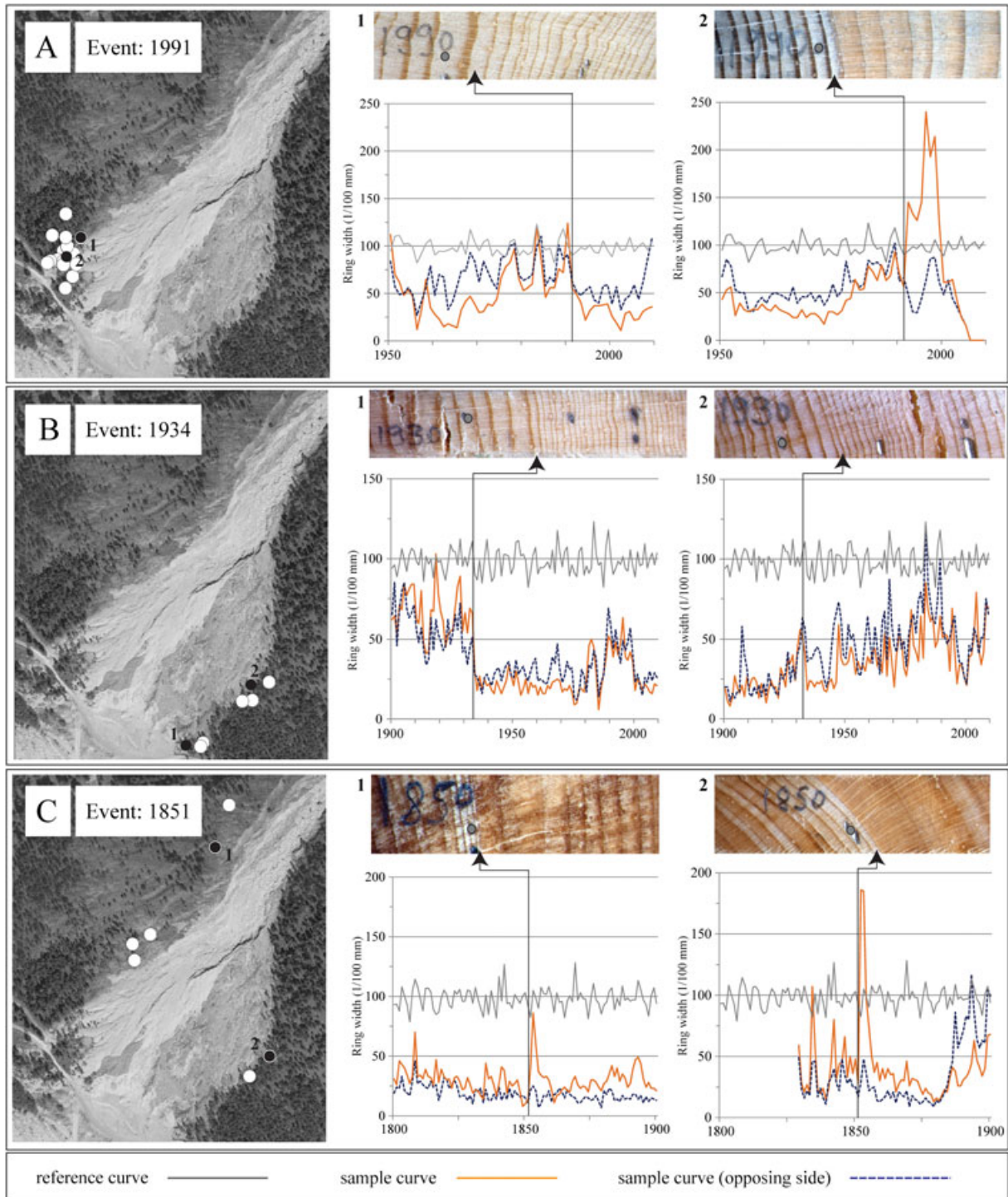
Figure 5. Example of event reconstruction using a calibration year (A, 1991) to exemplify growth disturbances (GDs) for the identification of additional historical events (B, 1934; C, 1851). Growth suppression as found in 1991 (A1, intensity T_m) can similarly be seen in 1934 (B1 and B2, intensity T_s). Compression wood as found in 1991 (A2, intensity T_m) can similarly be seen in 1851 (C1, intensity T_w; C2, intensity T_m). Corresponding ring-width measurements and reference curves are provided. The spatial distribution of those trees showing GDs in the given year (○) and the example trees (●) is provided in the orthophotos (orthophotos are property of Land Vorarlberg, 2010). This figure is available in colour online at wileyonlinelibrary.com/journal/espl

thereby affecting the trees. Most importantly, however, the tree-ring data provided continuous information in periods of time in which orthophotos were not available. Aerial photographs were not obtained in the 1990s; however, the events identified in 1991, 1994, and 1998 indicate that the migration of deposits further into sector B (which was apparent in the orthophoto of 2001) was well advanced already at this point. Similarly, there are no existing aerial photographs in the 1960s, but the event identified in 1961 shows debris-flow activity well into the lateral aspects of sector C, which cannot be seen in the orthophotos

before (1951) or after (1973) this time. The tree-ring data also provided information over 12 additional decades before orthophotos were available. The spatial distribution of affected trees shows a shift in areas of activity between 1839 and 1934. Earlier events affected trees in sector A (1839, 1851), including trees in the central and lateral aspects; there is no evidence of debris-flow activity to this extent into sector A since this time. Afterwards, debris-flow activity shifted to sector C (1878, 1934) and influenced trees in the lateral aspects of this area. Only the event of 1922 shows evidence of trees affected in both sector B and C,

Table V. Growth disturbances corresponding to past debris-flow events listed by year, type and intensity, with an indication of the corresponding weighted index, W_{it}

	GR				GS				CW				I	Sum					W_{it}
	T_w	T_m	T_s	Total	T_w	T_m	T_s	Total	T_w	T_m	T_s	Total	T_i	T_w	T_m	T_s	T_i	Total	
1839	9	1	—	10	—	—	—	0	—	—	—	0	0	9	1	0	0	10	4.24
1851	2	1	1	4	—	—	—	0	1	1	—	2	0	3	2	1	0	6	3.43
1878	1	1	2	4	—	—	—	0	—	—	—	0	0	1	1	2	0	4	1.63
1906	—	1	2	3	—	—	—	0	—	—	—	0	0	0	1	2	0	3	0.83
1922	12	6	1	19	—	—	—	0	—	—	—	0	0	12	6	1	0	19	13.17
1934	—	—	—	0	1	1	2	4	—	1	—	1	0	1	2	2	0	5	0.99
1948	7	2	—	9	2	1	—	3	—	—	—	0	0	9	3	0	0	12	2.46
1961	5	—	2	7	—	2	—	2	—	—	—	0	0	5	2	2	0	9	2.54
1968	3	1	1	5	—	1	—	1	—	—	—	0	0	3	2	1	0	6	0.99
1981	6	11	1	18	—	2	—	2	—	1	—	1	0	6	14	1	0	21	15.64
1987	7	4	4	15	1	2	—	3	—	—	—	0	1	8	6	4	1	19	16.00
1991	—	3	2	5	1	3	—	4	—	1	—	1	6	1	7	2	6	16	12.79
1994	1	4	3	8	—	—	—	0	—	—	—	0	0	1	4	3	0	8	2.78
1998	—	2	2	4	2	2	1	5	—	1	—	1	0	2	5	3	0	10	4.82
2003	3	1	—	4	2	3		5	—	—	—	0	0	5	4	0	0	9	1.86
2007	—	—	—	0	—	—	—	0	—	1	1	2	2	0	1	1	2	4	0.60
Sum[a]	56	38	21	115	9	17	3	29	1	6	1	8	9	66	61	25	9	161	5.30

Note: Growth disturbances are indicated as growth release (GR), growth suppression (GS), compression wood (CW) and injuries (I). Intensity is classified as weak (T_w), moderate (T_m), strong (T_s) and injuries (T_i) following the criteria in Table I. Derivation of the W_{it} is shown in the Methods section.
[a]The mean value is shown for the W_{it}.
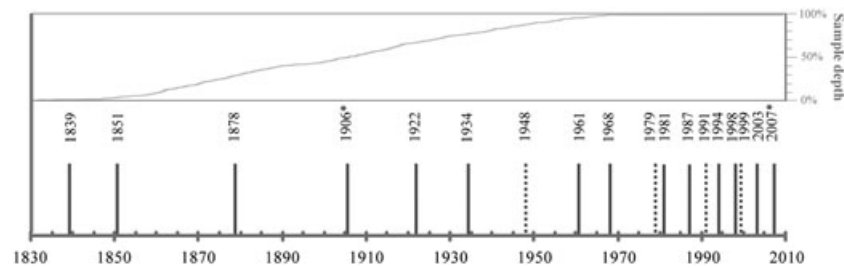
Figure 6. Frequency of reconstructed events including previously documented records (dashed line). Sample depth across the investigated time period is shown as a cumulative curve. Events with a W_{it} index < 0.99 are indicated with an asterisk.

suggesting either multiple events within this year or one larger event. Finally, the dendrogeomorphic analysis, as well as the orthophoto analysis, indicates that debris-flow activity since 1948 has primarily affected trees in sector B.

Discussion

In this study, we coupled orthophotos and tree-ring data to document spatial and temporal patterns of debris-flow activity on an active cone in the western Austrian Alps. Only through this integrative approach was it possible to gain a comprehensive understanding of debris-flow frequency and dynamics at this site, as well as to enable an estimation of the effect of tree loss on debris-flow reconstruction frequency.

The visual information obtained from the orthophotos was especially important for determining spatial extent of recent deposits and examining forest coverage on the cone. Small-scale features (e.g. small gullies between depositional lobes, incisions of the transport channels, game tracks) were also obvious and supported the interpretation of GDs found in the dendrogeomorphic assessment. The series of seven orthophotos was invaluable for quantifying singular tree loss over a short time period (1 yr), as well as general forest structure in cone sub-sectors over a longer time period. The evolution of depositional patterns since the 1950s was illustrated with higher

spatial resolution than was possible with dendrogeomorphic techniques at this site. However, dendrogeomorphic analysis enabled higher temporal resolution by specific dating of debris-flow events, which could be related to depositions visible in the orthophotos.

The dendrogeomorphic analysis also had limitations on this site. The ability to detect relevant GDs in the tree-ring series depends on both the characteristics of the deposited material and the tree species. The debris flows at Bärenrüfe have relatively low water content and contain small, granular material. As a result, the trees here are affected primarily by low-impact movements, meaning that stress to tree growth is mostly due to accumulative burial and not to high-impact injuries. This is seen from the predominance of growth suppression/release in the sample and the scarcity of injuries. In addition, the identification of GDs in PIUN trees is challenging for three reasons. Firstly, as these trees colonize sites where other species would not survive, growing conditions are already compromised under normal conditions and annual tree growth is minimal (mean 0.43 ± 0.35 mm, range $0.02–2.40$ mm for this sample), and less than other species on a similar site (Procter *et al.*, 2011). Secondly, it has been reported that other *Pinus* species are highly sensitive to soil dryness and nutrient deficiency in dolomitic sites (*Pinus sylvestris*, Central Austrian Alps; Oberhuber *et al.*, 1998) and to climatic factors, including temperature and precipitation (*Pinus cembra*, Central Austrian Alps;

Oberhuber, 2004; *Pinus cembra*, Central Swiss Alps; Vittoz *et al.*, 2008). Comparative growth curves obtained from trees on a similar but undisturbed site are helpful in differentiating climatic and geomorphic influences during GD analysis (Stoffel *et al.*, 2011). In this case, appropriate reference trees do not exist, as this species is found only in active or dormant deposition areas, and a reference growth curve had to be created from a prudent selection of trees within the sampled population (i.e. those least affected over the period of reconstruction). For this reason the use of a weighted index (W_{it}; Kogelnig-Mayer *et al.*, 2011) was valuable to incorporate a weighting of GD intensity and lessen the importance of number of affected trees. Thirdly, a growth release may be delayed due to fertilization effects of fine-grained, dolomitic material (Strunk, 1991; Stoffel *et al.*, 2008a), making it essential to identify event years primarily by injuries and high intensity, abrupt GDs (lower intensity reactions occurring in subsequent years should be evaluated cautiously). These issues, although discussed specifically for the Bärenrüfe site and PIUN trees, should be considered in any active debris-flow system that is characterized by repeated sedimentation events of lower intensity.

A further challenge in many active systems is the high degree of tree loss, with the consequence that potential records of past events are eliminated. The resulting reconstructed series on such sites have thus been defined as 'minimal frequency' records, i.e. not an exhaustive record of all events (Corona *et al.*, in press). But the question remains: how 'minimal' are they, i.e. what proportion of the actual debris-flow events were recorded in trees or, if present, were identified in the tree-ring analysis? One aspect influencing the analysis is the minimal number of trees showing GDs in coincident years required to define an event. Although a lower limit of 10 to 40% (i.e. percentage of existing trees showing GDs needed to define an event) has been used for dendrogeomorphic analyses of avalanches in the past (e.g. Butler and Malanson, 1985; Germain *et al.*, 2005; Luckman, 2010), defining such a threshold is not effective for debris flows due to a higher variability in event intensity and spatial extent and, therefore, a higher likelihood that a smaller area and fewer trees are affected (Stoffel and Bollschweiler, 2009b). This is visible, for example, in the range of W_{it} indices obtained in this sample. Nevertheless, the number of trees available for sampling will unavoidably determine the power of the analysis for identifying events. The results presented here show a tree loss of over 80% between 1951 and 2009; therefore, if < 20% of the trees were available for sampling compared to 1951, it could be speculated that < 20% of the more recent events were actually captured. If the nine events identified since 1951 represent 20% of the actual occurrences, the theoretical 100% would be 45 events, giving a return interval of 0·75 yr for a period of 60 years. Based on three annual field observations, it is evident that the Bärenrüfe catchment produces very frequent (< 1 yr), small (in the order of a few 10 to 100 m^3) debris flows with minor material relocation, suggesting that the frequency presented earlier may indeed be in a realistic range. Even if a dense forest cover was present in this segment of the cone in the past, not all *Pinus* trees are expected to register a disturbance by these very frequent, small debris flows. Based on deposits visible in the orthophotos as well as in the tree-ring data, most debris flows with higher return periods have probably been registered in at least some of the surviving trees, but this will not necessarily be maintained in future due to the continuously disappearing forest stand.

From a dendroecological perspective, such an excessive rate of tree death may be explained by the exceedance of some critical threshold in depositional depth (by individual or a series of events) after which tree die-off is accelerated (Strunk, 1997).

If more events have reached forested areas in recent decades, then there were either comparatively fewer events prior to this or earlier events came to rest higher on the cone. Field evidence exists for significant depositions at the cone apex, which have a much finer composition than recent deposits. Data from a high-elevation, transport-limited catchment in the Swiss Alps suggests that debris flows would have involved smaller volumes during the Little Ice Age (LIA) and that activity was much less frequent at that time compared to the early decades of the twentieth century (Stoffel and Beniston, 2006; Stoffel, 2010). As a consequence, smaller grain sizes were found preferentially in deposits and earlier deposition of material was observed on the fan (Stoffel *et al.*, 2008b). Comparable changes in the debris-flow system could possibly have created conditions favourable for the establishment of an old-growth forest during the LIA and, in contrast, created a new situation in the course of the twentieth century which is now leading to the elimination of this forest.

Conclusion

In active debris-flow systems with repeated sedimentation events, characterization of cone dynamics and event history can be a challenge due to both the inability to identify smaller, less intense events and the removal of forest stands through high impact events or repetitive burial of stems. A quantitative estimation of the degree to which dendrogeomorphic analyses are a 'minimal dating technique' is a pragmatic problem that is generally not directly addressed because of the difficulty of finding a system of measurement. Using high resolution data on forest coverage in a series of orthophotos, we have provided an estimation of this effect on this site. In areas of rapid tree loss, the use of a weighted index for identification of events is a highly valuable tool for incorporating the intensity of growth changes so as to avoid an undue focus on the mere number of affected trees. Further development and application of such indices would offer increased systematization and enable comparative analyses in dendrogeomorphic studies.

References

Alestalo J. 1971. Dendrochronological interpretation of geomorphic processes. *Fennia* **105**: 1–140.

Baroni C, Armiraglio S, Gentili R, Carton A. 2007. Landform-vegetation units for investigating the dynamics and geomorphic evolution of alpine composite debris cones (Valle dell'Avio, Adamello group, Italy). *Geomorphology* **84**: 59–79.

Blair T, McPherson JG. 1998. Recent debris-flow processes and resultant form and facies of the dolomite alluvial fan, Owens Valley, California. *Journal of Sedimentary Research* **68**(5): 800–818.

Butler DR, Malanson GP. 1985. A history of high-magnitude snow avalanches, southern Glacier National Park, Montana, USA. *Mountain Research and Development* **5**(2): 175–182.

Cavalli M, Marchi L. 2008. Characterisation of the surface morphology of an alpine alluvial fan using airborne LiDAR. *Natural Hazards and Earth System Sciences* **8**: 323–333.

Cavalli M, Tarolli P, Marchi L, Fontana GD. 2008. The effectiveness of airborne LiDAR data in the recognition of channel-bed morphology. *Catena* **73**: 249–260.

Corona C, Lopez Saez J, Stoffel M, Bonnefoy M, Richard D, Astrade L, Berger F. In press. How much of the real avalanche activity can be captured with tree rings? An evaluation of classic dendrogeomorphic approaches and comparison with historical archives. *Cold Regions Science and Technology*. DOI: http://dx.doi.org/10.1016/j.coldregions.2012.01.003

ESRI. 2008. ArcMap® software. http://www.esri.com/software/arcgis [1 March 2011].

Geologische Bundesanstalt. 2000. *Rocky Austria: A Brief Earth History of Austria*. Geological Survey of Austria: Vienna.

Germain D, Filion L, H'etu B. 2005. Snow avalanche activity after fire and logging disturbances, northern Gasp'e, Quebec, Canada. *Canadian Journal of Earth Sciences* **42**: 2103–2116.

Hydrographischer Dienst Vorarlberg. 2010. On-line and private database from the Hydrographischer Dienst Vorarlberg. http://gis.lebensministerium.at/eHYD [1 March 2011].

Kogelnig-Mayer B, Stoffel M, Bollschweiler M, Hübl J, Rudolf-Miklau F. 2011. Possibilities and limitations of dendrogeomorphic time-series reconstructions on sites influenced by debris flows and frequent snow avalanche activity. *Arctic, Antarctic, and Alpine Research* **43**: 649–658.

Land Vorarlberg. 2010. On-line and archival database from the Land Vorarlberg Landesvermessungsamt. http://www.vorarlberg.gv.at/vorarlberg/bauen_wohnen/bauen/landesvermessungsamt/start.htm [1 March 2011].

Luckman BH. 2010. Dendrogeomorphology and snow avalanche research. In *Tree-rings and Natural Hazards: A State-of-the-art*, Stoffel M, Bollschweiler M, Butler DR, Luckman BH (eds). Springer: Dordrecht; 27–34.

Marchi L, Cavalli M. 2007. Procedures for the documentation of historical debris flows: application to the Chieppena torrent (Italian Alps). *Environmental Management* **40**: 492–503.

Marchi L, Tecca PR. 2006. Some observations on the use of data from historical documents in debris-flow studies. *Natural Hazards* **38**: 301–320.

Mayer H. 1974. *Wälder des Ostalpenraum*. Gustav Fischer Verlag: Stuttgart.

Oberhuber W. 2004. Influence of climate on radial growth of *Pinus cembra* within the alpine timberline ecotone. *Tree Physiology* **24**: 291–301.

Oberhuber W, Stumböck M, Kofler W. 1998. Climate–tree–growth relationships of Scots pine stands (*Pinus sylvestris* L.) exposed to soil dryness. *Trees* **13**: 19–27.

Procter E, Bollschweiler M, Stoffel M, Neumann M. 2011. A regional reconstruction of debris-flow activity in the Northern Calcareous Alps, Austria. *Geomorphology* **132**: 41–50.

Rinntech. 2011. LINTAB Präzision – Jahrring für Jahrring. http://www.rinntech.com/content/view/16/47/lang [2 January 2011].

Scheidl C, Rickenmann D, Chiari M. 2008. The use of airborne LiDAR data for the analysis of debris flow events in Switzerland. *Natural Hazards and Earth System Sciences* **8**: 1113–1127.

Shroder JF. 1978. Dendrogeomorphological analysis of mass movement on Table Cliff Plateau, Utah. *Quaternary Research* **9**: 168–185.

Staley DM, Wasklewicz TA, Blaszczynski JS. 2006. Surficial patterns of debris flow deposition on alluvial fans in Death Valley, CA using airborne laser swath mapping data. *Geomorphology* **74**: 152–163.

Stoffel M. 2010. Magnitude–frequency relationships of debris flows – a case study based on field surveys and tree-ring records. *Geomorphology* **116**: 67–76.

Stoffel M, Beniston M. 2006. On the incidence of debris flows from the early Little Ice Age to a future greenhouse climate: a case study from the Swiss Alps. *Geophysical Research Letters* **33**: L16404.

Stoffel M, Bollschweiler M. 2008. Tree-ring analysis in natural hazards research – an overview. *Natural Hazards and Earth System Sciences* **8**: 187–202.

Stoffel M, Bollschweiler M. 2009a. What tree rings can tell about earth-surface processes: teaching the principles of dendrogeomorphology. *Geography Compass* **3**: 113–137.

Stoffel M, Bollschweiler M. 2009b. Tree-ring reconstruction of past debris flows based on a small number of samples – possibilities and limitations. *Landslides* **6**: 225–230.

Stoffel M, Bollschweiler M, Butler DR, Luckman BH. 2010. *Tree Rings and Natural Hazards: A State-of-the-art.* Springer: Heidelberg.

Stoffel M, Bollschweiler M, Leutwiler A, Aeby P. 2008a. Large debris-flow events and overbank sedimentation in the Illgraben torrent (Valais Alps, Switzerland). *Open Geology Journal* **2**: 18–29.

Stoffel M, Bollschweiler M, Vazquez-Selem L, Franco-Ramos O, Palacios D. 2011. Dendrogeomorphic dating of rockfalls on low-latitude, high-elevation slopes: Rodadero, Iztaccíhuatl volcano, Mexico. *Earth Surface Processes and Landforms* **36**: 1209–1217.

Stoffel M, Conus D, Grichting MA, Lièvre I, Maître G. 2008b. Unraveling the patterns of late Holocene debris-flow activity on a cone in the central Swiss Alps: chronology, environment and implications for the future. *Global and Planetary Change* **60**: 222–234.

Stoffel M, Wilford DJ. 2012. Hydrogeomorphic processes and vegetation: disturbance, process histories, dependencies and interactions. *Earth Surface Processes and Landforms* **37**: 9–22.

Strunk H. 1991. Frequency distribution of debris flows in the Alps since the Little Ice Age. *Zeitschrift für Geomorphologie* **83**: 71–81.

Strunk H. 1997. A 300 years history of debris flow activity in the Southern Alps: vegetation cover, soil depth, forest fire and overgrazing as controlling factors. *Paläoklimaforschung* **19**(ESF Special Issue 12): 223–232.

Theler D, Reynard E, Lambiel C, Bardou E. 2010. The contribution of geomorphological mapping to sediment transfer evaluation in small alpine catchments. *Geomorphology* **124**: 113–123.

Vittoz P, Rulence B, Largey T, Frelechoux F. 2008. Effects of climate and land-use change on the establishment and growth of Cembran Pine (*Pinus cembra* L.) over the altitudinal treeline ecotone in the Central Swiss Alps. *Arctic, Antarctic, and Alpine Research* **40**(1): 225–232.

Volker HX, Wasklewicz TA, Ellis MA. 2007. A topographic fingerprint to distinguish alluvial fan formative processes. *Geomorphology* **88**: 34–45.